



## Fluorination-induced magnetism in boron nitride nanotubes from ab initio calculations

Feng Li, Zhonghua Zhu, Xiangdong Yao, Gaoqing Lu, Mingwen Zhao, Yueyuan Xia, and Ying Chen

Citation: *Applied Physics Letters* **92**, 102515 (2008); doi: 10.1063/1.2894507

View online: <http://dx.doi.org/10.1063/1.2894507>

View Table of Contents: <http://scitation.aip.org/content/aip/journal/apl/92/10?ver=pdfcov>

Published by the [AIP Publishing](#)

---

### Articles you may be interested in

[Transverse dielectric properties of boron nitride nanotubes by ab initio electric field calculations](#)

*Appl. Phys. Lett.* **94**, 183110 (2009); 10.1063/1.3129170

[Transformation from chemisorption to physisorption with tube diameter and gas concentration: Computational studies on N H 3 adsorption in BN nanotubes](#)

*J. Chem. Phys.* **127**, 184705 (2007); 10.1063/1.2786112

[Diameter-dependent spin polarization of injected carriers in carbon-doped zigzag boron nitride nanotubes](#)

*Appl. Phys. Lett.* **89**, 123103 (2006); 10.1063/1.2348773

[Are fluorinated boron nitride nanotubes n -type semiconductors?](#)

*Appl. Phys. Lett.* **87**, 243113 (2005); 10.1063/1.2142290

[Magnetism in BN nanotubes induced by carbon doping](#)

*Appl. Phys. Lett.* **86**, 122510 (2005); 10.1063/1.1890477

---

The logo for AIP APL Photonics is displayed on a red background with a bright yellow sunburst effect. The letters 'AIP' are in a large, white, sans-serif font, followed by a vertical bar and the words 'APL Photonics' in a smaller, white, sans-serif font.

AIP | APL Photonics

*APL Photonics* is pleased to announce  
**Benjamin Eggleton** as its Editor-in-Chief



## Fluorination-induced magnetism in boron nitride nanotubes from *ab initio* calculations

Feng Li,<sup>1,2</sup> Zhonghua Zhu,<sup>3,a)</sup> Xiangdong Yao,<sup>3</sup> Gaoqing Lu,<sup>3</sup> Mingwen Zhao,<sup>4</sup> Yueyuan Xia,<sup>4</sup> and Ying Chen<sup>5</sup>

<sup>1</sup>Department of Physics, Taishan University, Taian, Shandong 271021, People's Republic of China

<sup>2</sup>Division of Chemical Engineering, School of Engineering, University of Queensland, Brisbane 4072, Australia

<sup>3</sup>Division of Chemical Engineering and ARC Centre of Excellence for Functional Nanomaterials, School of Engineering, University of Queensland, Brisbane 4072, Australia

<sup>4</sup>School of Physics and Microelectronics, Shandong University, Jinan, Shandong 250100, People's Republic of China

<sup>5</sup>Research School of Physical Sciences and Engineering, Australian National University, Canberra Australia Capital Territory 0200 Australia

(Received 23 November 2007; accepted 18 February 2008; published online 14 March 2008)

*Ab initio* calculations were conducted to investigate the electronic structures and magnetic properties of fluorinated boron nitride nanotube (F-BNNT). It was found that the chemisorption of F atoms on the B atoms of BNNT can induce spontaneous magnetization, whereas no magnetism can be produced when the B and N atoms are equally fluorinated. This provides a different approach to tune the magnetic properties of BNNTs as well as a synthetic route toward metal-free magnetic materials. © 2008 American Institute of Physics. [DOI: 10.1063/1.2894507]

Magnetism in metal-free materials has been the focus of extensive research recently because of the great potential application in spintronic devices. Since ferro- and ferrimagnetism were experimentally discovered in polymerized C<sub>60</sub> (Ref. 1) and proton-irradiated graphite,<sup>2</sup> considerable theoretical efforts have been devoted to investigate the origin of magnetism in metal-free materials and to search for materials with similar properties. Lehtinen *et al.*<sup>3,4</sup> performed *ab initio* calculations to study the properties of a carbon adatom on a graphite sheet and a carbon nanotube and found that the adatom is spin polarized in both cases. Fujita *et al.*<sup>5</sup> performed tight-binding band structure calculations on the graphite ribbons and predicted that spontaneous magnetization could appear in the graphite ribbons with armchair edges. Ma *et al.*,<sup>6</sup> on the basis of *ab initio* calculations, predicted that the vacancy defects can induce magnetism in graphite sheets and carbon nanotubes. For graphitic BN sheets and BN nanotubes (BNNTs),<sup>7,8</sup> the nitrogen vacancy or the boron vacancy can also induce spontaneous magnetization. The theoretical prediction of spontaneous magnetization in BNNTs induced by substituting carbon or silicon atoms for boron or nitrogen atoms has also been reported by several groups.<sup>9,10</sup> In addition, the hydrogenation treatment of carbon materials can also induce magnetism.<sup>11–13</sup> These theoretical studies provide useful theoretical guide for the experimental synthesis of these metal-free magnetic materials, which, however, remain challenging partially due to the difficulties in the controlled growth of these defects.

Recently, Tang *et al.*<sup>14</sup> succeeded in the preparation of stable fluorinated BNNTs (F-BNNTs) and found that their resistance and resistivity are about three orders of magnitude less than those of pure BNNTs, which are considered by several groups<sup>15–17</sup> to be due to the modified band structures of BNNTs induced by the adsorption and substitution of F atoms. However, the magnetic properties of these F-BNNTs

have not yet been studied neither experimentally nor theoretically. In this paper, we investigated the magnetic properties of F-BNNTs by performing spin-polarized density functional calculations. Our results show that the chemisorption of F atoms on B sites is more stable than that on N sites and can induce stable spontaneous magnetization in the F-BNNTs. This provides a different approach to tune the magnetic properties of BNNTs as well as a synthetic route toward metal-free magnetic materials.

All calculations were performed within the density functional theory, with spin polarization taken into account, as implemented in the SIESTA (Refs. 18–20) program. The pseudopotentials generated using the Trouiller and Martins scheme<sup>21</sup> were used to describe the interaction of valence electron with the atomic core and their nonlocal components were expressed in the fully separable form of Kleiman and Bylander.<sup>22,23</sup> The generalized gradient approximation correction in the form of Perdew *et al.*<sup>24</sup> was adopted for the exchange correlation potential. The atomic orbital basis set employed throughout was a double- $\zeta$  plus polarization orbital. The charge density was calculated in a regular real space grid with a cutoff energy of 120 Ry. Periodic boundary condition along the tube axis was employed and a vacuum region (at least 18.0 Å) between BNNTs was applied along the radial direction to avoid the mirror interactions between the tubes. Structural optimization was carried out for all of the configurations using the conjugate gradient algorithm until the residual forces were smaller than 0.02 eV/Å. A set of eight *k* points generated according to the Monkhorst–Pack scheme<sup>25</sup> was used to sample the Brillouin zone.

We conducted test calculations on F-(8,0) BNNT, F-(10,0) BNNT, F-(5,5) BNNT, and two-dimensional F-BN sheet; they have nearly the same magnetic behavior. Experiments have shown that BNNTs prefer a nonhelical or zigzag orientation during the growth.<sup>26</sup> Therefore, we focus on the magnetic behavior of (8,0) BNNT in this paper.

<sup>a)</sup>Electronic mail: z.zhu@uq.edu.au.

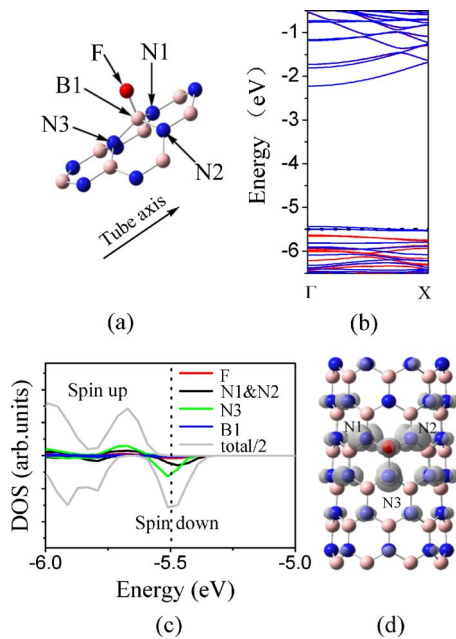


FIG. 1. (Color online) (a) The local map of F+B configuration near the adsorbing site. (b) The band structure of the F+B configuration. Red and blue lines represent spin-up and spin-down branches, respectively. The Fermi level is at 5.50 eV and is indicated by dotted line. (c) DOS and PDOS (only the more interesting contributions) of the F+B configuration. For clarity and convenience, the local maps near the Fermi level are presented and the DOS is scaled down. The Fermi level is indicated by dotted line. (d) The isosurface of the difference spin density at the isovalue of  $0.02 e/\text{\AA}^3$  for F+B. Red, blue, and pink balls represent F, N, and B atoms, respectively.

In our calculation, two sizes of supercells were employed for the F-(8,0) BNNT. One contains three primitive cells (96 atoms) where the distance between two adjacent F atoms is large enough to avoid the interactions between them, as shown in Fig. 1. Another consisting of two unit cells (64 atoms), as shown in Fig. 2, was adopted to study the adsorption of F atoms on (8,0) BNNT at the coverage of 25%.

We firstly considered the adsorption of a single F atom on a B or N atom of (8,0) BNNT. It was found that the F atom prefers to adsorb on a B atom [denoted as F+B, as shown in Fig. 1(a)], whereas the F adsorbed on a N atom will eventually transfer to a B atom during the structural optimization, which is consistent with the results of Xiang *et al.*<sup>15</sup>

For the purpose of comparison, we calculated the electronic structure of a pristine (8,0) BNNT. No spontaneous magnetization was found, suggesting that the pristine (8,0) BNNT is nonmagnetic. In contrast, the band structure of the F+B configuration [Fig. 1(b)] clearly shows that the spin-up and spin-down branches of the valence bands are split asymmetrically. The valence bands of the spin-up branch, which are all below the Fermi level, are fully occupied. The two bands of the spin-down branch, which cross over the Fermi level and are partially occupied, have an energy difference of 60 meV at the  $\Gamma$  point. The asymmetry between the spin-up and spin-down branches gives rise to spontaneous magnetization of this F-BNNT with a net magnetic moment of about  $0.99 \mu_B$ .

To understand the spontaneous magnetization, the spin density of states (DOS) of the F+B configuration and the projected DOSs (PDOS) for the mostly influenced atoms are plotted in Fig. 1(c). The spin-up peaks near the Fermi level are all below the Fermi level, whereas only one spin-down peak is crossed by the Fermi level. According to the previous discussion, the spin-down peak includes two electronic states, which, however, are not visible due to the Gaussian broadening applied to the DOS. It is found from the PDOS [Fig. 1(c)] that the spin-down peak mainly arises from the three N atoms (N1, N2, and N3) adjacent to the fluorinated B atom (B1) in Fig. 1(a). However, the contributions of F and B1 to the spin-down states are very small. Moreover, Mulliken population analysis shows that parts of charge on the highest-energy occupied  $2p$  orbitals of the N atoms around B1 move to the F atom which has a strong electronegative character. The total net spin ( $S=1/2$ ) mainly comes from the  $2p$  orbitals of the three N atoms adjacent to B1. The contributions of these nitrogen atoms N1, N2, and N3 to the magnetic moment are  $0.16 \mu_B$ ,  $0.16 \mu_B$ , and  $0.14 \mu_B$ , respectively. This is also consistent with the isosurfaces of the spin density ( $\Delta\rho = \rho_{\uparrow} - \rho_{\downarrow}$ ) of the F-BNNT, as shown in Fig. 1(d), where the net spin mainly localizes on the three N atoms around B1. We also calculated the energy of the paramagnetic state ( $S=0$ ) of the F-BNNT, finding that it is higher than that of the ferromagnetic state by about 87 meV.

From the application viewpoint, it is even more important to examine the magnetic properties of F-BNNTs at a higher F coverage. Zhou *et al.*<sup>17</sup> suggested that the coverage of F atoms on the external surface of BNNTs can be up to

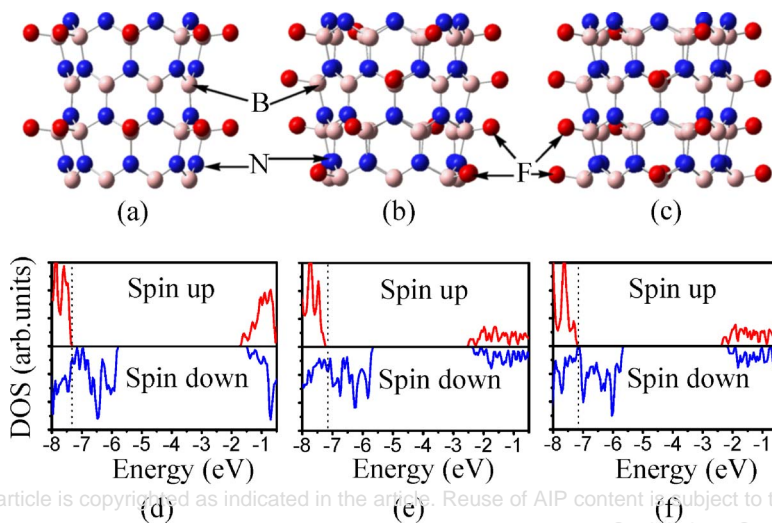


FIG. 2. (Color online) The optimized configurations and DOSs of fluorinated BN (8,0) nanotubes with F atoms adsorbing on B atoms in different ways: [(a) and (d)] for  $16F+B-1$ , [(b) and (e)] for  $16F+B-2$ , and [(c) and (f)] for  $16F+B-3$ . Red, blue, and pink balls represent F, N, and B atoms, respectively. The Fermi level is indicated by dotted line.



50% and all the F atoms favor the attachment to B atoms. In this work, we considered three isomeric configurations (16F+B-1, 16F+B-2, and 16F+B-3) of fluorinated (8,0) BNNT containing 16 F atoms in per supercell (equivalent to a coverage of 25%), as shown in Fig. 2. These F atoms are aligned over the B atoms on the exterior surface of the BNNT in different distributions. All of these structures are strongly magnetic with the magnetic moment as larger as  $16\mu_B$ . The 16F+B-2 and 16F+B-3 are energetically comparable with the energy difference less than 140 meV/F atom and both are more stable than 16F+B-1. It is noteworthy that the DOS of these configurations near the Fermi level are quite different [as shown in Figs. 2(d)–2(f)]. The Fermi level of 16F+B-3 lies between two states of spin-down branch with a gap of 0.21 eV, exhibiting the characters of spin semiconductors. For 16F+B-1 and 16F+B-2, however, the Fermi level crosses several states of spin-down branch and these materials can therefore be regarded as half metals.

Our calculations clearly show that the selective fluorination of BNNTs can induce magnetism in these tubes. Although, the F atoms adsorbed on the surface of BNNTs escape easily when the tubes are exposed to air or under standard beam irradiation in the electron microscope, the BNNTs with adsorbed F atoms can easily be obtained via a long-time direct reaction between BNNTs and fluorine or hydrogen fluoride at low temperature.<sup>14</sup> Therefore, if the metal catalysts, which are used to catalyze tubes growth, can be removed by chemical leaching process,<sup>27</sup> the magnetism of F-BNNTs can be discovered experimentally. F-BNNTs have good potential for spintronic applications, such as tunneling magnetoresistance and giant magnetoresistance elements, at low temperature.

In summary, we have performed *ab initio* local spin density approximation calculations to study the magnetic properties of F-BNNTs. We predict that the F adsorption on B atoms of the BNNTs can induce strong magnetism in BNNTs and the magnetic moment increases with the increasing F coverage. Compared to other metal-free magnets previously proposed, F-BNNTs can be easily synthesized and will have good potential in building spintronic devices.

This work was supported by the National Natural Science Foundation of China under Grant Nos. 10547131, 10674099, 50402017, and 10374059 and the National Basic Research 973 Program of China (Grant No. 2005CB623602).

Financial supports from ARC (Australian Research Council) linkage international fellowship grant and the University of Queensland Early Career funding are also appreciated. Feng Li also thanks Taishan University for the financial support.

- <sup>1</sup>T. L. Makarova, B. Sundqvist, R. Höhne, P. Esquinazi, Y. Kopelevich, P. Scharff, V. A. Davydov, L. S. Kashevarova, and A. V. Rakhmanina, *Nature (London)* **413**, 716 (2001).
- <sup>2</sup>P. Esquinazi, A. Setzer, R. Hohne, C. Semmelhack, Y. Kopelevich, D. Spemann, T. Butz, T. B. Kohlstrunk, and M. Losche, *Phys. Rev. B* **66**, 024429 (2002).
- <sup>3</sup>P. O. Lehtinen, A. S. Foster, A. Ayuela, A. Krashennnikov, K. Nordlund, and R. M. Nieminen, *Phys. Rev. Lett.* **91**, 017202 (2004).
- <sup>4</sup>P. O. Lehtinen, A. S. Foster, A. Ayuela, T. T. Vehviläinen, and R. M. Nieminen, *Phys. Rev. B* **69**, 155422 (2004).
- <sup>5</sup>M. Fujita, K. Wakabayashi, K. Nakata, and K. Kusakabe, *J. Phys. Soc. Jpn.* **65**, 1920 (1996).
- <sup>6</sup>Y. C. Ma, P. O. Lehtinen, A. S. Foster, and R. M. Nieminen, *New J. Phys.* **6**, 68 (2004).
- <sup>7</sup>M. S. Si and D. S. Xue, *Phys. Rev. B* **75**, 193409 (2007).
- <sup>8</sup>T. M. Schmidt, R. J. Baierle, P. Piquini, and A. Fazzio, *Phys. Rev. B* **67**, 113407 (2003).
- <sup>9</sup>R. Q. Wu, L. Liu, G. W. Peng, and Y. P. Feng, *Appl. Phys. Lett.* **86**, 122510 (2005).
- <sup>10</sup>M. S. Si and D. S. Xue, *Europhys. Lett.* **76**, 664 (2006).
- <sup>11</sup>K. Kusakabe and M. Maruyama, *Phys. Rev. B* **67**, 092406 (2003).
- <sup>12</sup>X. Y. Pei, X. P. Yang, and J. M. Dong, *Phys. Rev. B* **73**, 195417 (2006).
- <sup>13</sup>Y. C. Ma, P. O. Lehtinen, A. S. Foster, and R. M. Nieminen, *Phys. Rev. B* **72**, 085451 (2005).
- <sup>14</sup>C. Tang, Y. Bando, Y. Huang, S. Yue, C. Gu, F. Xu, and D. Golberg, *J. Am. Chem. Soc.* **127**, 6552 (2005).
- <sup>15</sup>H. J. Xiang, J. L. Yang, J. G. Hou, and Q. S. Zhu, *Appl. Phys. Lett.* **87**, 243113 (2005).
- <sup>16</sup>L. Lai, W. Song, J. Lu, Z. X. Gao, S. Nagase, M. Ni, W. N. Mei, J. J. Liu, D. P. Yu, and H. Q. Ye, *J. Phys. Chem. B* **110**, 14092 (2006).
- <sup>17</sup>Z. Zhou, J. J. Zhao, Z. F. Chen, and P. R. Schleyer, *J. Phys. Chem. B* **110**, 25678 (2006).
- <sup>18</sup>P. Ordejón, E. Artacho, and J. M. Soler, *Phys. Rev. B* **53**, R10441 (1996).
- <sup>19</sup>D. Sánchez-Portal, P. Ordejón, E. Artacho, and J. M. Soler, *Int. J. Quantum Chem.* **6**, 553 (1997).
- <sup>20</sup>J. M. Soler, E. Artacho, J. D. Gale, A. García, J. Junquera, P. Ordejón, and D. Sánchez-Portal, *J. Phys.: Condens. Matter* **14**, 2745 (2002), and references therein.
- <sup>21</sup>N. Troullier and J. L. Martins, *Phys. Rev. B* **43**, 1993 (1991).
- <sup>22</sup>L. Kleinman and D. M. Bylander, *Phys. Rev. Lett.* **48**, 1425 (1982).
- <sup>23</sup>D. M. Bylander and L. Kleinman, *Phys. Rev. B* **41**, 907 (1990).
- <sup>24</sup>J. Perdew, K. Burke, and M. Ernzerhof, *Phys. Rev. Lett.* **77**, 3865 (1996); **78**, 1396 (1997).
- <sup>25</sup>H. J. Monkhorst and J. D. Pack, *Phys. Rev. B* **13**, 5188 (1976).
- <sup>26</sup>D. Golberg, Y. Bando, L. Bourgeois, K. Kurashima, and T. Sato, *Appl. Phys. Lett.* **77**, 1979 (2000).
- <sup>27</sup>H. Chen, Y. Chen, J. Yu, and J. S. Williams, *Chem. Phys. Lett.* **425**, 315 (2006).